Numer. Math. Theor. Meth. Appl.
doi: 10.4208/nmtma.2015.m1331

Vol. **8**, No. 4, pp. 475-495
November 2015

A Numerical Method for Solving Matrix Coefficient Heat Equations with Interfaces

Liqun Wang[1] and Liwei Shi[2,*]

[1] *Department of Mathematics, China University of Petroleum (Beijing), Beijing, 102249, China.*
[2] *Department of Science and Technology Teaching, China University of Political Science and Law, Beijing, 102249, China.*

Received 02 November 2013; Accepted (in revised version) 04 July 2014

Abstract. In this paper, we propose a numerical method for solving the heat equations with interfaces. This method uses the non-traditional finite element method together with finite difference method to get solutions with second-order accuracy. It is capable of dealing with matrix coefficient involving time, and the interfaces under consideration are sharp-edged interfaces instead of smooth interfaces. Modified Euler Method is employed to ensure the accuracy in time. More than 1.5th order accuracy is observed for solution with singularity (second derivative blows up) on the sharp-edged interface corner. Extensive numerical experiments illustrate the feasibility of the method.

AMS subject classifications: 65N30

Key words: Heat equation, Sharp-edged interface, Jump condition, Matrix coefficient.

1. Introduction

Interface problems arise in problems involving multi-physics/multi-phase materials, which is common in fluid dynamics, electromagnetic, biological systems [1, 2], etc. Therefore, they attract considerable interest both theoretically and numerically in the past decades. However, due to the low global regularity and the irregular geometry of the interface, it is difficult to design a highly efficient method for such problems. In this paper, we seek the solution for heat equations with sharp-edged interface and matrix coefficient. The setting of the problem is as follows:

Consider a rectangular domain $\Omega = (x_{min}, x_{max}) \times (y_{min}, y_{max})$. Γ is an interface prescribed by the zero level-set $\{(x, y) \in \Omega \mid \phi(x, y) = 0\}$ of a level-set function $\phi(x, y)$.

*Corresponding author. *Email addresses:* wliqunhmily@gmail.com (L.-Q. Wang), sliweihmily@gmail.com (L.-W. Shi)

 ©2015 Global-Science Press

https://doi.org/10.4208/nmtma.2015.m1331 Published online by Cambridge University Press

The unit normal vector of Γ is $\boldsymbol{n} = \frac{\nabla\phi}{|\nabla\phi|}$ pointing from $\Omega^- = \{(x,y) \in \Omega \mid \phi(x,y) \leq 0\}$ to $\Omega^+ = \{(x,y) \in \Omega \mid \phi(x,y) \geq 0\}$. Now the governing equation reads

$$\frac{\partial u(\boldsymbol{x},t)}{\partial t} - \bigtriangledown \cdot (\beta(\boldsymbol{x},t) \bigtriangledown u(\boldsymbol{x},t)) = f(\boldsymbol{x},t), \text{ in } (\Omega \setminus \Gamma) \times (0,T), \tag{1.1}$$

in which $\boldsymbol{x} = (x_1, ..., x_d)$ denotes the spatial variables and $\bigtriangledown$ is the gradient operator. The coefficient $\beta(\boldsymbol{x},t)$ is assumed to be a $d \times d$ matrix that is uniformly elliptic on each disjoint subdomain, Ω^- and Ω^+, and its components are continuously differentiable on each disjoint subdomain, but they may be discontinuous across the interface Γ. The right-hand side $f(\boldsymbol{x},t)$ is assumed to lie in $L^2(\Omega)$.

Given functions a and b along the interface Γ, we prescribe the jump conditions on $\Gamma \times (0,T)$

$$\begin{aligned} &[u(\boldsymbol{x},t)]_\Gamma \equiv u^+(\boldsymbol{x},t) - u^-(\boldsymbol{x},t) = a(\boldsymbol{x},t), \\ &[(\beta(\boldsymbol{x},t) \bigtriangledown u(\boldsymbol{x},t)) \cdot \boldsymbol{n}]_\Gamma \equiv \boldsymbol{n} \cdot (\beta^+(\boldsymbol{x},t) \bigtriangledown u^+(\boldsymbol{x},t)) \\ &\qquad\qquad - \boldsymbol{n} \cdot (\beta^-(\boldsymbol{x},t) \bigtriangledown u^-(\boldsymbol{x},t)) = b(\boldsymbol{x},t), \end{aligned} \tag{1.2}$$

The superscripts "$\pm$" refer to limits taken from within the subdomains $\Omega^\pm$. Finally, we prescribe initial and boundary conditions

$$\begin{aligned} &u(\boldsymbol{x},0) = u_0(\boldsymbol{x}), \text{ in } \Omega, \\ &u(\boldsymbol{x},t) = g(\boldsymbol{x},t), \text{ on } \partial\Omega \times (0,T). \end{aligned} \tag{1.3}$$

for a given function g on the boundary $\partial\Omega$ and u_0 on the domain Ω.

Since the pioneer work of Peskin in 1977, much attention has been paid to solving interface problems. The Immersed Boundary Method [3, 4] that he proposed uses a numerical approximation of the δ-function, which smears out the solution on a thin finite band around the interface Γ. In [5], the "immersed boundary" method was combined with the level set method, resulting in a first order numerical method that is simple to implement, even in multiple spatial dimensions. However, for both methods, the numerical smearing at the interface forces continuity of the solution at the interface, regardless of the interface condition $[u] = a$, where a might not be zero.

After that, in order to get higher order accuracy, researchers has done a lot of work on the finite difference solution for interface problems. The main idea is to use difference scheme and stencils carefully near the interface to incorporate jump conditions and achieve high order local truncation error using Taylor expansion. The Immersed Interface Method [6, 7] incorporates the interface conditions into the finite difference scheme near the interface to achieve second-order accuracy based on a Taylor expansion in a local coordinate system. The corresponding linear system is sparse, but not symmetric or positive definite.

The Boundary Condition Capturing Method [8] uses the idea of Ghost Fluid Method [9] to capture the boundary conditions. The method extends the solution from one side across the interface using the jump conditions. The GFM is robust and simple to

https://doi.org/10.4208/nmtma.2015.m1331 Published online by Cambridge University Press

implement, and so is the resulting boundary condition capturing method. In [10], the boundary condition capturing method has been sped up by a multi-grid method. The method can solve the elliptic equation with interface conditions $[u] \neq 0$ and $[\beta u_{\boldsymbol{n}}] \neq 0$ in two and three dimensions. However, the original version is only first order accurate. In a recent work [11], the method is improved to second order accuracy for smooth interfaces.

In [12], the Matched Interface and Boundary Method was proposed to solve elliptic equations with smooth interfaces. In [13], the matched interface and boundary method was generalized to treat sharp-edged interfaces. With an elegant treatment, second order accuracy was achieved in the L^∞ norm. However, for oscillatory solutions, the errors deteriorate.

The existing finite element schemes on non-body-fitted meshes are usually designed by modifying the finite element basis near the interface. Examples of finite element methods for interface problems are Extended Finite Element Method [14–16], Immersed Finite Element Method [17, 18], and Penalty Finite Element Method [19, 20]. Chen and Zou [21] studied the convergence of the finite element method for elliptic and parabolic interface problems, sub-optimal error estimates can be achieved for smooth interfaces. The convergence of Immersed Finite Element Method for semi-linear parabolic interface problems was analyzed in [22], which proved that the convergence rates for the semi-discrete and fully discrete schemes based on the backward Euler method are in the optimal order.

In [23], a non-traditional finite element formulation for solving elliptic equations with smooth or sharp-edged interfaces was proposed with non-body-fitting grids for $[u] \neq 0$ and $[\beta u_{\boldsymbol{n}}] \neq 0$. It achieved second order accuracy in the L^∞ norm for smooth interfaces and about 0.8-th order for sharp-edged interfaces. In [24, 25], the method is modified and improved to close to 2nd order accurate for sharp-edged interfaces, and it is extended to handle general elliptic equations with matrix coefficient and lower order terms. The resulting linear system is non-symmetric but positive definite.

Also, there has been a large body of work from the finite volume perspective for developing high order methods for elliptic and parabolic interface problems. Colella and collaborators proposed the Embedded Boundary Method (EBM) [26–28] from the finite volume perspective, which embeds the domain into a regular Cartesian grid. In [29], this method was extended to parabolic problems with fixed or moving interfaces in domains with complex geometry. This method can achieve second-order accuracy in both space and time.

In this paper, based on our previous work [24, 25, 30–35], we propose a new numerical method for solving the heat equations with interfaces. Generally speaking, this method uses different basis for the test function and the jump conditions across the interface, which are standard finite element basis and piecewise linear basis, respectively. The Modified Euler Method is employed to get second-order accuracy in time. Compared with [6, 36], this method has two advantages: first, this method is capable of dealing with a larger variety of interfaces, including sharp-edged interface and complex interface; second, the coefficients are generalized to matrix instead of scalar and

https://doi.org/10.4208/nmtma.2015.m1331 Published online by Cambridge University Press

the time term can be included in the matrix, which obviously enlarged the scope of problem that can be solved. Numerical experiments show that this method can achieve second-order accuracy.

2. Weak formulation

First, define some notations, see [21,37]. For a Banach space B, define

$$H^m(0,T;B)=\Big\{u(t)\in B \text{ for a.e. } t\in(0,T) \text{ and } \|u\|_{H^m(0,T;B)}<\infty\Big\},$$

where $\| u \|_{H^m(0,T;B)}$ is the norm of $H^m(0,T;B)$ and is given by

$$\|u\|_{H^m(0,T;B)}=\left\{\sum_{k=0}^{m}\int_0^T \|u^{(k)}(t)\|_B^2 dt\right\}^{1/2},$$
$$L^2(0,T;B)=H^0(0,T;B).$$

In the rest of this section, we derive the weak formulation of the interface problem. To this end, we split it into two heat equations:

$$\frac{\partial u^+(\boldsymbol{x},t)}{\partial t}-\nabla\cdot(\beta(\boldsymbol{x},t)\nabla u^+(\boldsymbol{x},t))=f(\boldsymbol{x},t),\quad \text{in } \Omega^+\times[0,T], \tag{2.1}$$
$$\frac{\partial u^-(\boldsymbol{x},t)}{\partial t}-\nabla\cdot(\beta(\boldsymbol{x},t)\nabla u^-(\boldsymbol{x},t))=f(\boldsymbol{x},t),\quad \text{in } \Omega^-\times[0,T], \tag{2.2}$$

Note that the boundary of each subdomain $\partial\Omega^{\pm}$ is Lipschitz continuous, and thus integration by parts is valid on each subdomain [38, Theorem 1.5.3.1].

Now we are ready to derive the weak formulations for (2.1) and (2.2). First, by multiplying both sides of (1.1) with the test function $\psi\in H_0^1(\Omega)$ and integrating over the subdomain Ω^+, we deduce from Green's theorem that

$$\begin{aligned}\int_{\Omega^+} f\psi &= \int_{\Omega^+}\frac{\partial u}{\partial t}\psi-\int_{\Omega^+}\nabla\cdot(\beta\nabla u)\psi\\ &=\int_{\Omega^+}\frac{\partial u}{\partial t}\psi+\int_{\Omega^+}\beta\nabla u\cdot\nabla\psi-\int_{\Omega^+\bigcap\partial\Omega}\beta^+\psi\frac{\partial u^+}{\partial \boldsymbol{n}^+}-\int_{\Gamma}\beta^+\psi\frac{\partial u^+}{\partial \boldsymbol{n}^+},\end{aligned} \tag{2.3}$$

where $\boldsymbol{n}^+$ is the unit outward normal direction of $\partial\Omega^+$. Similarly, we have

$$\int_{\Omega^-} f\psi=\int_{\Omega^-}\frac{\partial u}{\partial t}\psi+\int_{\Omega^-}\beta\nabla u\cdot\nabla\psi-\int_{\Omega^-\bigcap\partial\Omega}\beta^-\psi\frac{\partial u^-}{\partial \boldsymbol{n}^-}-\int_{\Gamma}\beta^-\psi\frac{\partial u^-}{\partial \boldsymbol{n}^-}, \tag{2.4}$$

where $\boldsymbol{n}^-$ is the unit outward normal direction of $\partial\Omega^-$. On the interface Γ, we set the normal direction $\boldsymbol{n}$ point from Ω^- to Ω^+ such that $\boldsymbol{n}=\boldsymbol{n}^-=-\boldsymbol{n}^+$. We note that if $\Omega^-\cap\partial\Omega$ is an empty set, then

$$\int_{\Omega^-\cap\partial\Omega}\beta^-\psi\frac{\partial u^-}{\partial \boldsymbol{n}^-}=0.$$

https://doi.org/10.4208/nmtma.2015.m1331 Published online by Cambridge University Press

Otherwise, we have $\psi|_{\partial\Omega} = 0$ because $\psi \in H_0^1(\Omega)$, so

$$\int_{\Omega^+ \bigcap \partial\Omega} \beta^+ \psi \frac{\partial u^+}{\partial \boldsymbol{n}^+} = 0 \quad \text{and} \quad \int_{\Omega^- \bigcap \partial\Omega} \beta^- \psi \frac{\partial u^-}{\partial \boldsymbol{n}^-} = 0.$$

Adding Eq. (2.4) and Eq. (2.3) gives the weak formulation for the heat Eq. (1.1): for any $\psi \in H_0^1(\Omega)$

$$\begin{aligned}\int_\Omega f\psi &= \int_{\Omega^+} f\psi + \int_{\Omega^-} f\psi \\ &= \int_{\Omega^+} (\frac{\partial u}{\partial t}\psi + \beta\nabla u \cdot \nabla\psi) + \int_{\Omega^-} (\frac{\partial u}{\partial t}\psi + \beta\nabla u \cdot \nabla\psi) - \int_\Gamma (\beta^+\psi\frac{\partial u^+}{\partial \boldsymbol{n}^+} - \beta^-\psi\frac{\partial u^-}{\partial \boldsymbol{n}^-}) \\ &= \int_{\Omega^+} \frac{\partial u}{\partial t}\psi + \int_{\Omega^-} \frac{\partial u}{\partial t}\psi + \int_{\Omega^+} \beta\nabla u \cdot \nabla\psi + \int_{\Omega^-} \beta\nabla u \cdot \nabla\psi + \int_\Gamma b\psi. \end{aligned} \tag{2.5}$$

3. Numerical method

Below we employ the weak formulation for the heat equation. First divide the time interval $[0, T]$ into N equally spaced subintervals $[t_{n-1}, t_n], n = 1, 2, \cdots, N$, with $t_n = n\Delta t, \Delta t = T/N$.

According to the improved Euler method in [39], (1.1) can be rewritten as

$$\frac{\partial u(\boldsymbol{x}, t_{n+1/2})}{\partial t} - \bigtriangledown \cdot (\beta(\boldsymbol{x}, t_{n+1/2}) \bigtriangledown u(\boldsymbol{x}, t_{n+1/2})) = f(\boldsymbol{x}, t_{n+1/2}), \quad n = 1, \cdots, N, \tag{3.1}$$

where $t_{n+1/2} = (t_n + t_{n+1})/2$.

The Taylor series expansions of u^{n+1} and u^n at $t_{n+1/2}$ are given by

$$u(\boldsymbol{x}, t_{n+1}) = u(\boldsymbol{x}, t_{n+1/2} + \Delta t/2) = u(\boldsymbol{x}, t_{n+1/2}) + \frac{\Delta t}{2}\frac{du(\boldsymbol{x}, t_{n+1/2})}{dt} + O(\Delta t^2), \tag{3.2}$$

$$u(\boldsymbol{x}, t_n) = u(\boldsymbol{x}, t_{n+1/2} - \Delta t/2) = u(\boldsymbol{x}, t_{n+1/2}) - \frac{\Delta t}{2}\frac{du(\boldsymbol{x}, t_{n+1/2})}{dt} + O(\Delta t^2). \tag{3.3}$$

By subtracting (3.3) from (3.2), we have

$$\frac{du(\boldsymbol{x}, t_{n+1/2})}{dt} = (u(\boldsymbol{x}, t_{n+1}) - u(\boldsymbol{x}, t_n))/2 + O(\Delta t^2), \tag{3.4}$$

and by adding (3.3) to (3.2), we deduce

$$u(\boldsymbol{x}, t_{n+1/2}) = (u(\boldsymbol{x}, t_n) + u(\boldsymbol{x}, t_{n+1}))/2 + O(\Delta t^2), \tag{3.5}$$

Now by substituting (3.4) and (3.5) into (3.1) and taking into account the truncation error, the following semidiscrete problem by the modified Euler method is derived:

$$\begin{aligned}&\frac{u(\boldsymbol{x}, t_{n+1}) - u(\boldsymbol{x}, t_n)}{\Delta t} - \bigtriangledown \cdot (\beta(\boldsymbol{x}, t_{n+1/2}) \bigtriangledown \frac{u(\boldsymbol{x}, t_{n+1}) + u(\boldsymbol{x}, t_n)}{2}) \\ &= f(\boldsymbol{x}, t_{n+1/2}), \quad n = 1, \cdots, N.\end{aligned}$$

https://doi.org/10.4208/nmtma.2015.m1331 Published online by Cambridge University Press

Now the weak formulation of semidiscrete problem reads

$$\int_{\Omega^+}(u^{n+1}\psi+\frac{\Delta t}{2}\beta^{n+1/2}\nabla u^{n+1}\cdot\nabla\psi)+\int_{\Omega^-}(u^{n+1}\psi+\frac{\Delta t}{2}\beta^{n+1/2}\nabla u^{n+1}\cdot\nabla\psi)$$
$$=\int_{\Omega^+}(u^{n}\psi-\frac{\Delta t}{2}\beta^{n+1/2}\nabla u^{n}\cdot\nabla\psi)+\int_{\Omega^-}(u^{n}\psi-\frac{\Delta t}{2}\beta^{n+1/2}\nabla u^{n}\cdot\nabla\psi)$$
$$+\Delta t\int_\Omega f^{n+1/2}\psi-\Delta t\int_\Gamma b^{n+1/2}\psi,\qquad\forall\psi\in H_0^1(\Omega),$$

where

$$b^{n+1/2}=\boldsymbol{n}\cdot(\beta^{+,n+1/2}\bigtriangledown u^{+,n+1/2})-\boldsymbol{n}\cdot(\beta^{-,n+1/2}\bigtriangledown u^{-,n+1/2}).$$

For ease of discussion, and for the numerical test in Section 4, we assume that the functions a and b are smooth on the closure of Ω, β and f are smooth on $\Omega^+\times(0,T)$ and $\Omega^-\times(0,T)$, but they may be discontinuous across the interface Γ. However the boundaries $\partial\Omega$, $\partial\Omega^-$ and $\partial\Omega^+$ are always Lipschitz continuous. We assume that there is a Lipschitz continuous and piecewise smooth level-set function ϕ on Ω, where $\Gamma=\{\phi=0\}$, $\Omega^-=\{\phi<0\}$ and $\Omega^+=\{\phi>0\}$. A unit vector $\boldsymbol{n}=\frac{\bigtriangledown\phi}{|\bigtriangledown\phi|}$ can be obtained on $\overline{\Omega}$, which is a unit normal vector of Γ pointing from Ω^- to Ω^+.

In this paper, we restrict ourselves to a rectangular domain $\Omega=(x_{min},x_{max})\times(y_{min},y_{max})$ in the plane, β is a 2×2 matrix that is uniformly elliptic in each subdomain. Given positive integers I and J, set $\Delta x=(x_{max}-x_{min})/I$ and $\Delta y=(y_{max}-y_{min})/J$. Define $(x_i,y_j)=(x_{min}+i\Delta x,y_{min}+j\Delta y)$ for $i=0,...,I$ and $j=0,...,J$ as a uniform Cartesian grid. Each (x_i,y_j) is called a grid point. For the case $i=0,I$ or $j=0,J$, a grid point is called a boundary point, otherwise it is called an interior point. The grid size is defined as $h=max(\Delta x,\Delta y)>0$.

Two sets of grid functions are needed and they are denoted by

$$H_\pm^{1,h}=\Big\{\omega^h=(\omega_{i,j}):0\le i\le I,0\le j\le J\Big\},$$
$$H_0^{1,h}=\Big\{\omega^h=(\omega_{i,j})\in H_\pm^{1,h}:\omega_{i,j}=0\ \texttt{if}\ i=0,I\ \texttt{or}\ j=0,J\Big\}.$$

Next we cut every rectangular region $[x_i,x_{i+1}]\times[y_j,y_{j+1}]$ into two right triangles: one is bounded by $x=x_i,y=y_j$ and $y=\frac{y_{j+1}-y_j}{x_i-x_{i+1}}(x-x_{i+1})+y_j$, the other is bounded by $x=x_{i+1},y=y_{j+1}$ and $y=\frac{y_{j+1}-y_j}{x_i-x_{i+1}}(x-x_{i+1})+y_j$. Collecting all those triangular regions, we obtain a uniform triangulation $T^h:\bigcup_{K\in T^h}K$, see Fig. 1. We can also choose the hypotenuse to be $y=\frac{y_{j+1}-y_j}{x_{i+1}-x_i}(x-x_i)+y_j$, and get another uniform triangulation from the same Cartesian grid. There is no conceptual difference on these two triangulations for our method.

If $\phi(x_i,y_j)\le0$, we count the grid point (x_i,y_j) as in $\overline{\Omega^-}$; otherwise we count it as in Ω^+. An edge of a triangle in the triangulation is called an interface edge if the two vertices belong to different subdomains; otherwise we call it a regular edge.

A cell K is called an interface cell if its vertices belong to different subdomains. In an interface cell, we write $K=K^+\bigcup K^-$. K^+ and K^- are separated by a straight

https://doi.org/10.4208/nmtma.2015.m1331 Published online by Cambridge University Press

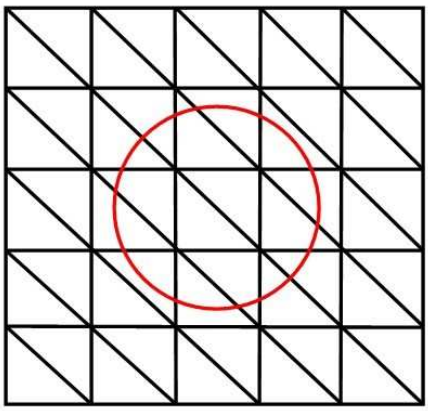


Figure 1: A uniform triangulation.

line segment, denoted by Γ_K^h. The two end points of the line segment Γ_K^h are located on interface Γ and their locations are calculated from the linear interpolations of the discrete level-set functions $\phi^h = \phi(x_i, y_j)$. The vertices of K^+ are located in $\Omega^+ \bigcup \Gamma$ and the vertices of K^- are located in $\Omega^- \bigcup \Gamma$. K^+ and $K^-$are approximations of the regions $K \bigcap \Omega^+$ and $K \bigcap \Omega^-$, respectively. A cell K is called a regular cell if all its vertices belong to the same subdomain, either Ω^+ or Ω^-. For a regular cell, we also write $K = K^+ \bigcup K^-$, where $K^- = \{\}$ (empty set) if all vertices of K are in Ω^+, and $K^+ = \{\}$ if all vertices of K are in Ω^-. Clearly $\Gamma_K^h = \{\}$ in a regular cell, K^+ and K^- are approximations of the regions $K \bigcap \Omega^+$ and $K \bigcap \Omega^-$, respectively. We use $|K^+|$ and $|K^-|$ to represent the areas of K^+ and K^-, respectively.

Two extension operators are needed. The first extension operator is $T^h : H_{\pm}^{1,h} \rightarrow H_0^1(\Omega)$. For any $\psi^h \in H_0^{1,h}$, $T^h(\psi^h)$ is a standard continuous piecewise linear function, which is a linear function in every triangular cell and $T^h(\psi^h)$ matches ψ^h on grid points. Clearly such a function set, denoted by $H_0^{1,h}$, is a finite dimensional subspace of $H_0^1(\Omega)$. The second extension operator U^h is constructed as follows. For any $u^{h,n} \in H_{\pm}^{1,h}$ with $u^{h,n} = g^{h,n}$ on boundary points at t_n, $U^h(u^{h,n})$ is a piecewise linear function and matches $u^{h,n}$ on grid points at t_n. It is a linear function in each regular cell, just like the first extension operator $U^h(u^{h,n}) = T^h(u^{h,n})$ in a regular cell at t_n. In each interface cell, it consists of two pieces of linear functions, one is on K^+ and the other is on K^-. The location of its discontinuity in the interface cell is the straight line segment Γ_K^h. Note that two end points of the line segment are located on interface Γ, hence the interface condition $[u(t_n)] = a(t_n)$ could be and is enforced exactly at these two end points. In each interface cell, the interface condition $[\beta(t_n) \bigtriangledown u(t_n) \cdot \boldsymbol{n}] = b(t_n)$ is enforced with value b at the middle point of Γ_K^h. In order to use this extension, we need the following theorem.

Theorem 3.1. *For all $u^{h,n} \in H_{\pm}^{1,h}, U^h(u^{h,n})$ can be constructed uniquely at t_n, provided $T^h, \phi, a(t_n)$ and $b(t_n)$ are given.*

Proof. There are five different cases in consideration:

https://doi.org/10.4208/nmtma.2015.m1331 Published online by Cambridge University Press

Case 0. The cell $K_{1,2,3}$ is a regular triangle. When calculating, we assume that all vertices of the triangle belong to Ω^+ or Ω^-.

Suppose that vertices 1,2,3 of $K_{1,2,3}$ belong to Ω^-, then $K_{1,2,3} \subset \Omega^-$.

$$U^h(u^{h,n}) = u^n(x_1, y_1) + u_x^{-,n}(x - x_1) + u_y^{-,n}(y - y_1), \quad x, y \in K_{1,2,3},$$

where $u_x^{-,n}, u_y^{-,n}$ can be written in the following form

$$u_x^{-,n} = c_{x,1}^{-,n} u^{-,n}(1) + c_{x,2}^{-,n} u^{-,n}(2) + c_{x,3}^{-,n} u^{-,n}(3),$$
$$u_y^{-,n} = c_{y,1}^{-,n} u^{-,n}(1) + c_{y,2}^{-,n} u^{-,n}(2) + c_{y,3}^{-,n} u^{-,n}(3).$$

Case 1. The interface comes across one vertex of the cell $K_{1,2,3}$, see Fig. 2(a). When calculating, we need to check whether the vertex is on the interface or not. If it is on the interface, then it belongs to Ω^+, otherwise it depends on which domain it belongs to.

Suppose that vertices 2, 3 in Fig. 2(a) belong to Ω^-, $K_{1,2,3} \subset \Omega^-$.

$$U^h(u^{h,n}) = u^n(x_2, y_2) + u_x^{-,n}(x - x_2) + u_y^{-,n}(y - y_2), \quad x, y \in K_{1,2,3},$$

$u_x^{-,n}, u_y^{-,n}$ can be written in the following form

$$u_x^{-,n} = c_{x,1}^{-,n} u^{+,n}(1) + c_{x,2}^{-,n} u^{-,n}(2) + c_{x,3}^{-,n} u^{-,n}(3) + c_{x,4}^{-,n} a^n(1),$$
$$u_y^{-,n} = c_{y,1}^{-,n} u^{+,n}(1) + c_{y,2}^{-,n} u^{-,n}(2) + c_{y,3}^{-,n} u^{-,n}(3) + c_{y,4}^{-,n} a^n(1).$$

Case 2. The interface covers one side of the cell $K_{1,2,3}$, see Fig. 2(b). When calculating, we need to check whether one vertex is on the interface or not. If it is on the interface, then it belongs to Ω^+, otherwise it depends on which domain it belongs to. The difference between Cases 1 and 2 is that when calculating the integration, Case 1 does not need to calculate the line integration, but Case 2 does.

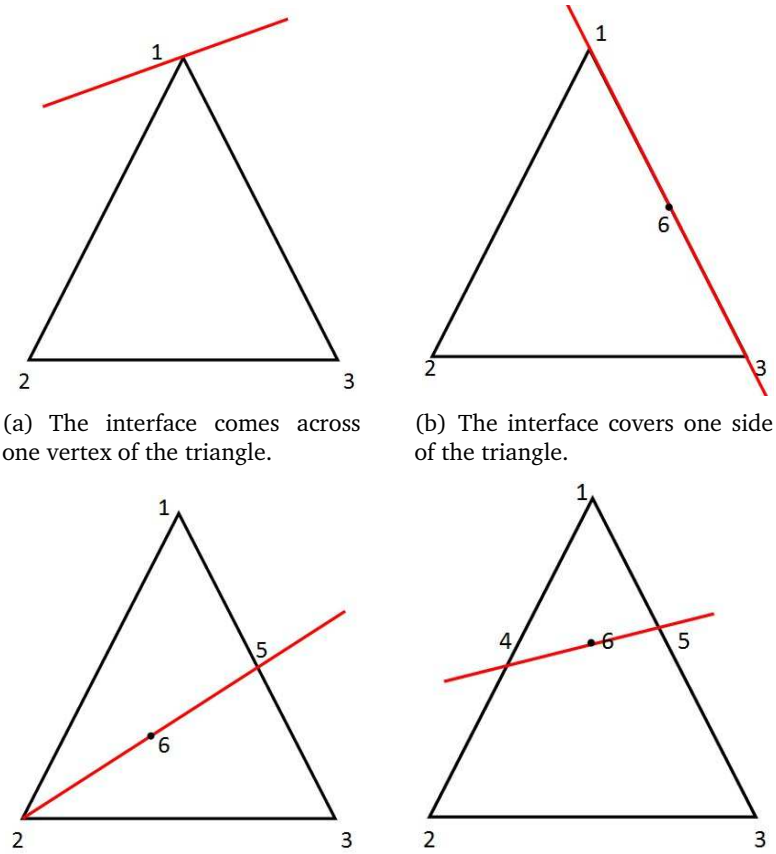
Suppose that vertex 2 in Fig. 2(b) belongs to Ω^-, $K_{1,2,3} \subset \Omega^-$.

$$U^h(u^{h,n}) = u^n(x_2, y_2) + u_x^{-,n}(x - x_2) + u_y^{-,n}(y - y_2), \quad x, y \in K_{1,2,3},$$

$u_x^{-,n}, u_y^{-,n}$ can be written in the following form

$$\begin{aligned} u_x^{-,n} = {} & c_{x,1}^{-,n} u^{+,n}(1) + c_{x,2}^{-,n} u^{-,n}(2) + c_{x,3}^{-,n} u^{+,n}(3) + c_{x,4}^{-,n} a^n(1) \\ & + c_{x,5}^{-,n} a^n(3) + c_{x,6}^{-,n} b^n(6), \\ u_y^{-,n} = {} & c_{y,1}^{-,n} u^{+,n}(1) + c_{y,2}^{-,n} u^{-,n}(2) + c_{y,3}^{-,n} u^{+,n}(3) + c_{y,4}^{-,n} a^n(1) \\ & + c_{y,5}^{-,n} a^n(3) + c_{y,6}^{-,n} b^n(6). \end{aligned}$$

https://doi.org/10.4208/nmtma.2015.m1331 Published online by Cambridge University Press



(a) The interface comes across one vertex of the triangle.

(b) The interface covers one side of the triangle.

(c) The interface comes across one vertex and one side of the triangle.

(d) The interface cuts two sides of the triangle.

Figure 2: Interface cells.

Case 3. The interface comes across one vertex and cuts one side of the cell $K_{1,2,3} = K^+ \bigcup K^-$, see Fig. 2(c). When calculating, we also need to check whether one vertex is on the interface or not. If it is on the interface, then it belongs to Ω^+, otherwise it depends on which domain it belongs to.

Suppose that vertex 1 in Fig. 2(c) belongs to Ω^+, then $K_{1,2,5} \subset \Omega^+$, vertex 3 in Fig. 2(c) belongs to Ω^-, then $K_{2,3,5} \subset \Omega^-$.

$$U^h(u^{h,n}) = \begin{cases} u^n(x_1, y_1) + u_x^{+,n}(x - x_1) + u_y^{+,n}(y - y_1), & x, y \in K_{1,2,5}, \\ u^n(x_3, y_3) + u_x^{-,n}(x - x_3) + u_y^{-,n}(y - y_3), & x, y \in K_{2,3,5}. \end{cases}$$

The value $u(5)^{\pm,n}$ of vertex 5 can be denoted as a linear function of $u^{+,n}(1)$, $u^{+,n}(2)$, $u^{-,n}(3)$,

$$u(5)^{+,n} = c_1^{+,n}u(1)^{+,n} + c_2^{+,n}u(2)^{+,n} + c_3^{+,n}u^{-,n}(3) + c_4^{+,n}a^n(2) + c_5^{+,n}a^n(5) + c_6^{+,n}b^n(6),$$
$$u(5)^{-,n} = c_1^{-,n}u(1)^{+,n} + c_2^{-,n}u(2)^{+,n} + c_3^{-,n}u^{-,n}(3) + c_4^{-,n}a^n(2) + c_5^{-,n}a^n(5) + c_6^{-,n}b^n(6).$$

https://doi.org/10.4208/nmtma.2015.m1331 Published online by Cambridge University Press

Hence $u_x^{-,n}, u_y^{-,n}, u_x^{+,n}$ and $u_y^{+,n}$ can be written in the following form

$$u_x^{+,n} = c_{x,1}^{+,n}u^{+,n}(1) + c_{x,2}^{+,n}u^{+,n}(2) + c_{x,3}^{+,n}u^{-,n}(3) + c_{x,4}^{+,n}a^n(2) + c_{x,5}^{+,n}a^n(5) + c_{x,6}^{+,n}b^n(6),$$

$$u_y^{+,n} = c_{y,1}^{+,n}u^{+,n}(1) + c_{y,2}^{+,n}u^{+,n}(2) + c_{y,3}^{+,n}u^{-,n}(3) + c_{y,4}^{+,n}a^n(2) + c_{y,5}^{+,n}a^n(5) + c_{y,6}^{+,n}b^n(6),$$

$$u_x^{-,n} = c_{x,1}^{-,n}u^{+,n}(1) + c_{x,2}^{-,n}u^{+,n}(2) + c_{x,3}^{-,n}u^{-,n}(3) + c_{x,4}^{-,n}a^n(2) + c_{x,5}^{-,n}a^n(5) + c_{x,6}^{-,n}b^n(6),$$

$$u_y^{-,n} = c_{y,1}^{-,n}u^{+,n}(1) + c_{y,2}^{-,n}u^{+,n}(2) + c_{y,3}^{-,n}u^{-,n}(3) + c_{y,4}^{-,n}a^n(2) + c_{y,5}^{-,n}a^n(5) + c_{y,6}^{-,n}b^n(6).$$

Case 4. The interface cuts two sides of the cell $K_{1,2,3} = K^+ \bigcup K^-$, see Fig. 2(d). When computing the integral, we need to check which domain one vertex belongs to.

Suppose that vertex 1 in Fig. 2(d) belongs to Ω^+, then $K_{1,4,5} \subset \Omega^+$, vertices 2, 3 in Fig. 2(d) belongs to Ω^-, then $K_{2,3,5} \subset \Omega^-$.

$$U^h(u^{h,n}) = \begin{cases} u^n(x_1, y_1) + u_x^{+,n}(x - x_1) + u_y^{+,n}(y - y_1), & x, y \in K_{1,2,5}, \\ u^n(x_3, y_3) + u_x^{-,n}(x - x_3) + u_y^{-,n}(y - y_3), & x, y \in K_{2,3,5}. \end{cases}$$

The value $u(4)^{\pm,n}$ and $u(5)^{\pm,n}$ can be represented as a linear function of $u^{+,n}(1)$, $u^{-,n}(2)$, $u^{-,n}(3)$,

$$u(4)^{+,n} = c_{4,1}^{+,n}u^{+,n}(1) + c_{4,2}^{+,n}u^{-,n}(2) + c_{4,3}^{+,n}u^{-,n}(3) + c_{4,4}^{+,n}a^n(4) + c_{4,5}^{+,n}a^n(5) + c_{4,6}^{+,n}b^n(6),$$

$$u(4)^{-,n} = c_{4,1}^{-,n}u^{+,n}(1) + c_{4,2}^{-,n}u^{-,n}(2) + c_{4,3}^{-,n}u^{-,n}(3) + c_{4,4}^{-,n}a^n(4) + c_{4,5}^{-,n}a^n(5) + c_{4,6}^{-,n}b^n(6),$$

$$u(5)^{+,n} = c_{5,1}^{+,n}u^{+,n}(1) + c_{5,2}^{+,n}u^{-,n}(2) + c_{5,3}^{+,n}u^{-,n}(3) + c_{5,4}^{+,n}a^n(4) + c_{4,5}^{+,n}a^n(5) + c_{4,6}^{+,n}b^n(6),$$

$$u(5)^{-,n} = c_{5,1}^{-,n}u^{+,n}(1) + c_{5,2}^{-,n}u^{-,n}(2) + c_{5,3}^{-,n}u^{-,n}(3) + c_{5,4}^{-,n}a^n(4) + c_{4,5}^{-,n}a^n(5) + c_{4,6}^{-,n}b^n(6).$$

Hence $u_x^{-,n}, u_y^{-,n}, u_x^{+,n}$ and $u_y^{+,n}$ can be written in the following form

$$u_x^{+,n} = c_{x,1}^{+,n}u^{+,n}(1) + c_{x,2}^{+,n}u^{-,n}(2) + c_{x,3}^{+,n}u^{-,n}(3) + c_{x,4}^{+,n}a^n(4) + c_{x,5}^{+,n}a^n(5) + c_{x,6}^{+,n}b^n(6),$$

$$u_y^{+,n} = c_{y,1}^{+,n}u^{+,n}(1) + c_{y,2}^{+,n}u^{-,n}(2) + c_{y,3}^{+,n}u^{-,n}(3) + c_{y,4}^{+,n}a^n(4) + c_{y,5}^{+,n}a^n(5) + c_{y,6}^{+,n}b^n(6),$$

$$u_x^{-,n} = c_{x,1}^{-,n}u^{+,n}(1) + c_{x,2}^{-,n}u^{-,n}(2) + c_{x,3}^{-,n}u^{-,n}(3) + c_{x,4}^{-,n}a^n(4) + c_{x,5}^{-,n}a^n(5) + c_{x,6}^{-,n}b^n(6),$$

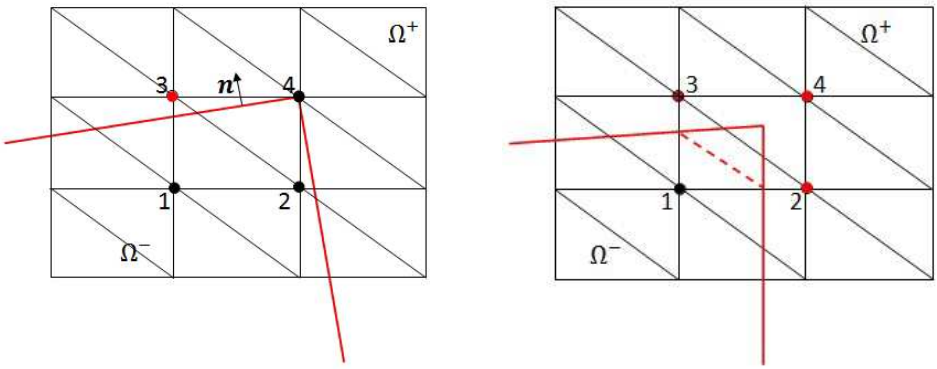
$$u_y^{-,n} = c_{y,1}^{-,n}u^{+,n}(1) + c_{y,2}^{-,n}u^{-,n}(2) + c_{y,3}^{-,n}u^{-,n}(3) + c_{y,4}^{-,n}a^n(4) + c_{y,5}^{-,n}a^n(5) + c_{y,6}^{-,n}b^n(6).$$

To complete the proof of Theorem 3.1, we need the following lemma [24]:

Lemma 3.1. *All coefficients c^n in Theorem* 3.1 *are finite and independent of $u^{h,n}, a^n$ and b^n.* □

Remark 3.1. For special cases when the sharp edge of the interface cut through the vertex or edges of a grid cell, take the red line in Fig. 3(a) for example, in irregular

https://doi.org/10.4208/nmtma.2015.m1331 Published online by Cambridge University Press



(a) (b)

Figure 3: Treatment of special cases.

cell Δ_{234}, the normal direction is perpendicular to the red line (interface) at the middle point, pointing from Ω^- to Ω^+; for special cases like the interface shown as the red line in figure Fig. 3(b), since red points 2 and 3 both belong to Ω^+, black point 1 belongs to Ω^-, in Δ_{123} the interface is dealt as the dashed line, Δ_{123} is treated as an irregular cell. For this reason, the interface would not appear in Δ_{234}, and it is treated as a regular cell.

Based on the above discussion, we propose the following method:

Method 3.1. Find a discrete function $u^{h,n} \in H_{\pm}^{1,h}$ with $u^{h,n} = g^{h,n}$ on boundary points such that for all $\psi^h \in H_0^{1,h}$, we have

$$\begin{aligned}
&\sum_{K\in T^h}\left(\frac{\Delta t}{2}\int_{K^+}\beta^{n+\frac{1}{2}}\bigtriangledown U^h(u^{h,n+1})\cdot\bigtriangledown T^h(\psi^h)+\int_{K^+}U^h(u^{h,n+1})T^h(\psi^h)\right.\\
&\quad\left.+\frac{\Delta t}{2}\int_{K^-}\beta^{n+\frac{1}{2}}\bigtriangledown U^h(u^{h,n+1})\cdot\bigtriangledown T^h(\psi^h)+\int_{K^-}U^h(u^{h,n+1})T^h(\psi^h)\right)\\
=&\sum_{K\in T^h}\left(\int_{K^+}U^h(u^{h,n})T^h(\psi^h)-\frac{\Delta t}{2}\int_{K^+}\beta^{n+\frac{1}{2}}\bigtriangledown U^h(u^{h,n})\cdot\bigtriangledown T^h(\psi^h)\right.\\
&\quad+\int_{K^-}U^h(u^{h,n})T^h(\psi^h)-\frac{\Delta t}{2}\int_{K^-}\beta^{n+\frac{1}{2}}\bigtriangledown U^h(u^{h,n})\cdot\bigtriangledown T^h(\psi^h)\\
&\quad\left.+\Delta t\int_{K^+}f^{n+\frac{1}{2}}T^h(\psi^h)+\Delta t\int_{K^-}f^{n+\frac{1}{2}}T^h(\psi^h)-\Delta t\int_{\Gamma_K^h}b^{n+\frac{1}{2}}T^h(\psi^h)\right).
\end{aligned}$$

To implement the method, we use the Gaussian quadrature rule for integrals. The idea is illustrated in Fig. 4. If T is separated into two pieces by the interface $\overline{u_4u_5}$, connect u_3 and u_4 to get three triangles: $T_1 = \triangle u_1u_4u_5$, $T_2 = \triangle u_2u_3u_4$, $T_3 = \triangle u_3u_4u_5$. For each triangle, label the center point p_{ij} of each edge $\overline{u_iu_j}$. In numerical computation, apply

https://doi.org/10.4208/nmtma.2015.m1331 Published online by Cambridge University Press

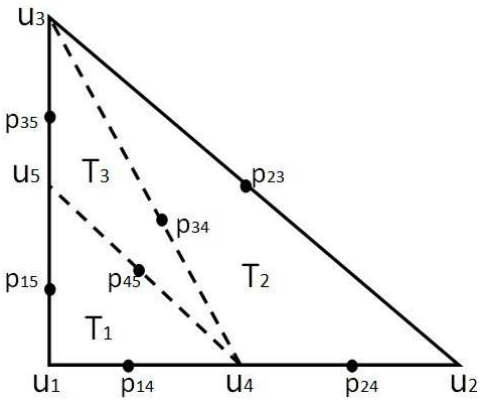


Figure 4: Quadrature.

the average of three $f(p_{ij})$ in each triangle. Numerical results show the quadrature can yield higher accuracy than that in [23].

4. Numerical experiments

In all numerical experiments below, the level-set function $\phi(x,y)$, the coefficients $\beta^{\pm}(x,y,t)$ and the solutions

$$\begin{aligned} u &= u^+(x,y,t), \qquad \texttt{in } \Omega^+ \times (0,T), \\ u &= u^-(x,y,t), \qquad \texttt{in } \Omega^- \times (0,T), \end{aligned}$$

are given. Hence

$$\begin{aligned} &u_0(x,y) = u^+(x,y,0), \ \ \texttt{in } \Omega^+; \quad u_0(x,y) = u^-(x,y,0), \ \ \texttt{in } \Omega^-, \\ &g(x,y,t) = u(x,y,t), \quad \texttt{on } \partial\Omega \times (0,T), \\ &f(x,y,t) = -\nabla \cdot (\beta(x,y,t)\nabla u(x,y,t)), \quad \texttt{in } \Omega \times (0,T), \\ &a(x,y,t) = u^+(x,y,t) - u^-(x,y,t), \quad \texttt{on } \Gamma \times (0,T), \\ &b(x,y,t) = \Big(\beta^+(x,y,t)\nabla u^+(x,y,t)\Big) \cdot \boldsymbol{n} \\ &\qquad\qquad - \Big(\beta^-(x,y,t)\nabla u^-(x,y,t)\Big) \cdot \boldsymbol{n}, \quad \texttt{on } \Gamma \times (0,T). \end{aligned}$$

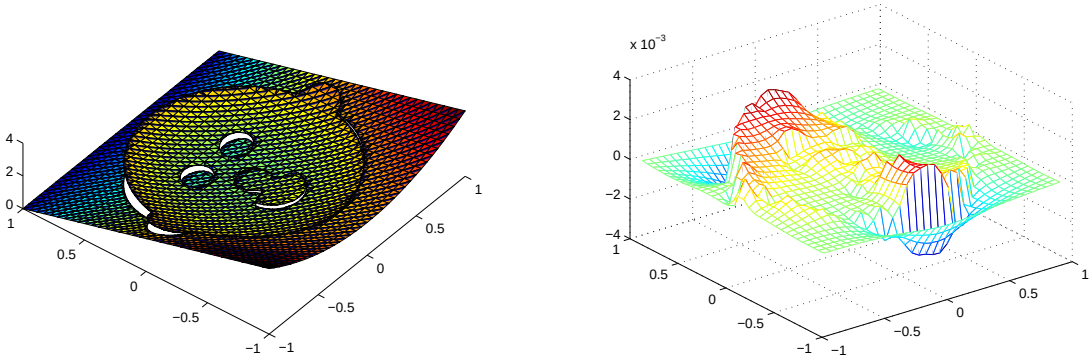
All the examples are defined on the domain $[-1,1] \times [-1,1] \times [0,1]$. All errors in solutions are measured in the L^∞ norm in the whole domain Ω.

Example 4.1. This example is a "happy face" interface. The level-set function ϕ, the coefficients $\beta^{\pm}$ and the solution $u^{\pm}$ are given as follows:

https://doi.org/10.4208/nmtma.2015.m1331 Published online by Cambridge University Press

Table 1: Happy Face

$n_x \times n_y \times n_t$	$\|u - u^h\|_\infty$	Order
$9 \times 9 \times 10$	0.035	
$18 \times 18 \times 20$	0.0098	1.82
$36 \times 36 \times 40$	0.0026	1.92
$72 \times 72 \times 80$	6.83e-004	1.93



(a) (b)

Figure 5: Happy Face.

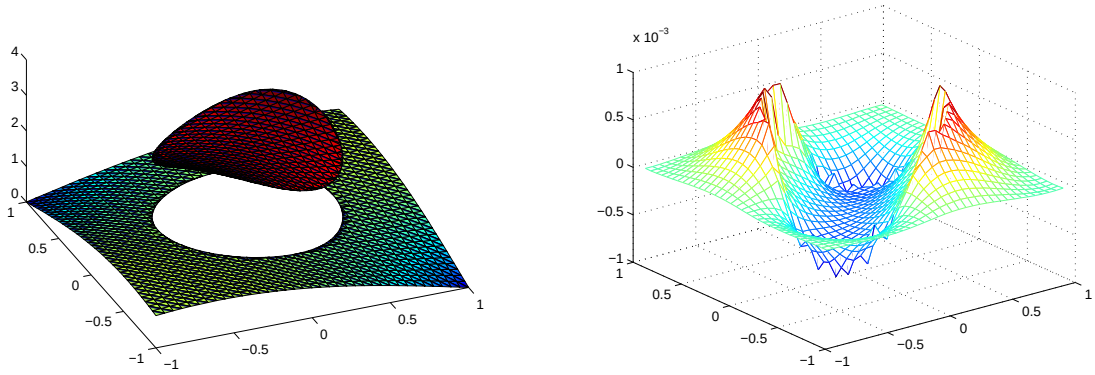
$$\phi(x,y) = \max(\min(\phi_1,\phi_2,\phi_3),\phi_4,\phi_5,\phi_6,\min(\phi_7,\phi_8)),$$
$$\phi_1(x,y) = x^2 + y^2 - 0.75^2 - 0.15^2,$$
$$\phi_2(x,y) = (x-0.75)^2 + y^2 - 0.15^2,$$
$$\phi_3(x,y) = (x+0.75)^2 + y^2 - 0.15^2,$$
$$\phi_4(x,y) = -\frac{0.1}{0.12}(x-0.2)^2 - \frac{0.12}{0.1}(y-0.22)^2 + 0.12\cdot 0.1,$$
$$\phi_5(x,y) = -\frac{0.1}{0.12}(x+0.2)^2 - \frac{0.12}{0.1}(y-0.22)^2 + 0.12\cdot 0.1,$$
$$\phi_6(x,y) = -x^2 - (y+0.08)^2 + 0.12^2,$$
$$\phi_7(x,y) = -x^2 - (y+0.625)^2 + 0.425^2,$$
$$\phi_8(x,y) = -x^2 - (y+0.25)^2 + 0.2^2,$$
$$\beta^+(x,y,t) = [x+5,0;0,2+xy],$$
$$\beta^-(x,y,t) = [y+2,0;0,0.5(x+y)+8],$$
$$u^+(x,y,t) = (1+x^2t)(1-y),$$
$$u^-(x,y,t) = \exp(x^2+y^2t).$$

Fig. 5(a) shows the numerical result at $t = 1$ using a $36 \times 36 \times 40$ grid. Fig. 5(b) shows the error of this example at $t = 1$ using a $36 \times 36 \times 40$ grid. Table 1 shows

https://doi.org/10.4208/nmtma.2015.m1331 Published online by Cambridge University Press

Table 2: Circle

$n_x \times n_y \times n_t$	$\|u - u^h\|_\infty$	Order
$9 \times 9 \times 10$	0.012	
$18 \times 18 \times 20$	0.0032	1.89
$36 \times 36 \times 40$	8.48e-004	1.91
$72 \times 72 \times 80$	2.34e-004	1.86



(a) (b)

Figure 6: Circle.

that the method achieves 2nd order accuracy on different grids for heat equations with sharp-edged interfaces when the matrix coefficients are functions of x and y.

Example 4.2. This example is a "circle" interface. The level-set function ϕ, the coefficients $\beta^{\pm}$ and the solution $u^{\pm}$ are given as follows:

$$\begin{aligned}
&\phi(x,y) = x^2 + y^2 - 0.563^2,\\
&\beta^+(x,y,t) = [tx + 6, x + 1 + t/5; x + 1 + t/5, 2t + xy + 5],\\
&\beta^-(x,y,t) = [t + y + 5, y + 1 + t/5; y + 1 + t/5, x + y + t + 6],\\
&u^+(x,y,t) = \sin(xy + t),\\
&u^-(x,y,t) = \exp(xy + t).
\end{aligned}$$

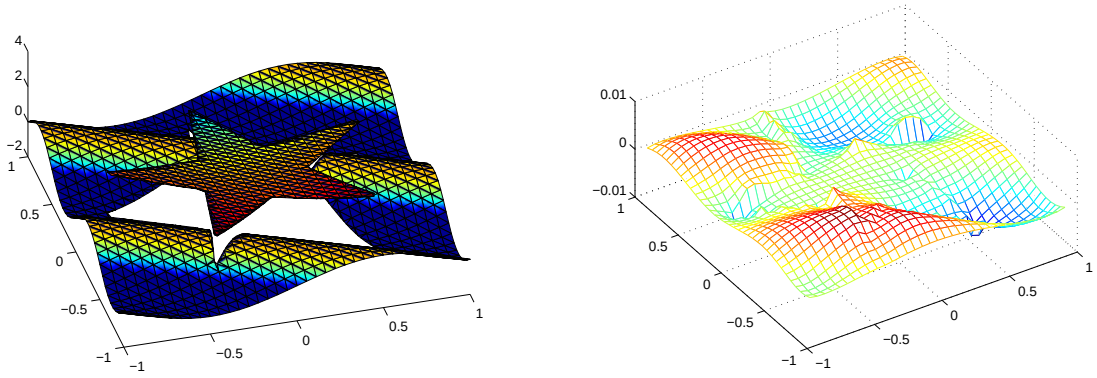
Fig. 6(a) shows the numerical result at $t = 1$ using a $36 \times 36 \times 40$ grid. Fig. 6(b) shows the error of this example at $t = 1$ using a $36 \times 36 \times 40$ grid. Table 2 shows that the method achieves 2nd order accuracy on different grids when the matrix coefficients are functions of x, y and t.

Example 4.3. This example is a "star" interface. The level-set function ϕ, the coeffi-

https://doi.org/10.4208/nmtma.2015.m1331 Published online by Cambridge University Press

Table 3: Star

$n_x \times n_y \times n_t$	$\|u - u^h\|_\infty$	Order
$9 \times 9 \times 10$	0.15	
$18 \times 18 \times 20$	0.040	1.87
$36 \times 36 \times 40$	0.0090	2.16
$72 \times 72 \times 80$	0.0022	2.02



(a) (b)

Figure 7: Star.

cients $\beta^{\pm}$ and the solution $u^{\pm}$ are given as follows:

$$\phi(r,\theta) = \begin{cases} \dfrac{R\sin(\frac{\theta_t}{2})}{\sin(\frac{\theta_t}{2} + \theta - \theta_r - \frac{2\pi(i-1)}{5})} - r, & \theta_r + \dfrac{\pi(2i-2)}{5} \le \theta < \theta_r + \dfrac{\pi(2i-1)}{5}, \\ \dfrac{R\sin(\frac{\theta_t}{2})}{\sin(\frac{\theta_t}{2} - \theta + \theta_r - \frac{2\pi(i-1)}{5})} - r, & \theta_r + \dfrac{\pi(2i-3)}{5} \le \theta < \theta_r + \dfrac{\pi(2i-2)}{5}, \end{cases}$$

with $\theta_t = \pi/5,\ \theta_r = \pi/7,\ R = 6/7$ and $i = 1, 2, 3, 4, 5$.

$$\beta^+(x,y,t) = [x + 5 + 2t, 0; 0, (2 + xy) + t],$$

$$\beta^-(x,y,t) = [y + 2 + t, 0; 0, 0.5(x + y) + 8 + tx],$$

$$u^+(x,y,t) = (1 + x^2 t)(1 - y),$$

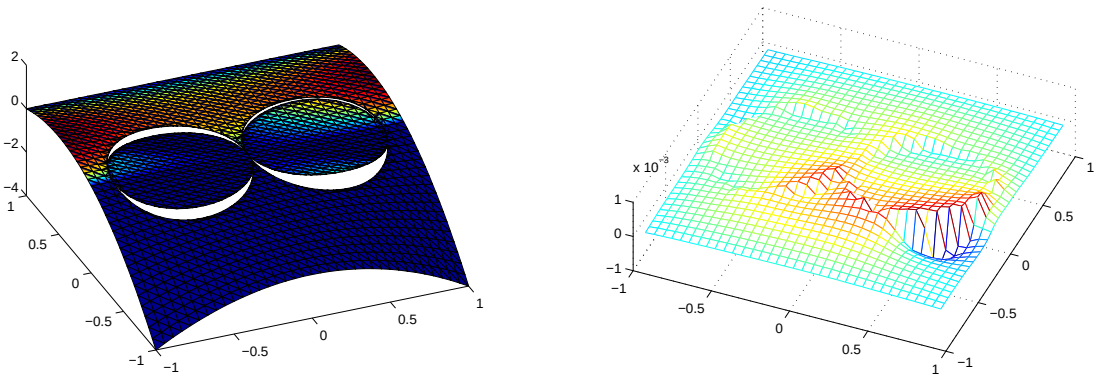
$$u^-(x,y,t) = \sin(\pi x + 2t\pi y).$$

Fig. 7(a) shows the numerical result at $t = 1$ using a $36 \times 36 \times 40$ grid. Fig. 7(b) shows the error of this example at $t = 1$ using a $36 \times 36 \times 40$ grid. Table 3 shows that the method achieves 2nd order accuracy on different grids for heat equations with sharp-edged interfaces when the matrix coefficients are functions of x, y and t.

https://doi.org/10.4208/nmtma.2015.m1331 Published online by Cambridge University Press

Table 4: Combination of Two Circles

$n_x \times n_y \times n_t$	$\|u - u^h\|_\infty$	Order
$9 \times 9 \times 10$	0.011	
$18 \times 18 \times 20$	0.0033	1.72
$36 \times 36 \times 40$	8.87e-004	1.89
$72 \times 72 \times 80$	2.28e-004	1.95



(a) (b)

Figure 8: Combination of Two Circles.

Example 4.4. The level-set function ϕ, the coefficients $\beta^{\pm}$ and the solution $u^{\pm}$ are given as follows:

$$\phi(x,y) = \min(\phi_1(x,y), \phi_2(x,y)),$$
$$\phi_1(x,y) = (x-0.431)^2 + y^2 - 0.431^2,$$
$$\phi_2(x,y) = (x+0.431)^2 + y^2 - 0.431^2,$$
$$\beta^+(x,y,t) = [x+2, 0; 0, 2+xy],$$
$$\beta^-(x,y,t) = [y+2, 0; 0, 0.5(x+y)+2],$$
$$u^+(x,y,t) = t^2(1+x^2)y(1-y),$$
$$u^-(x,y,t) = t^2 \sin(x+2y)\sin(xy).$$

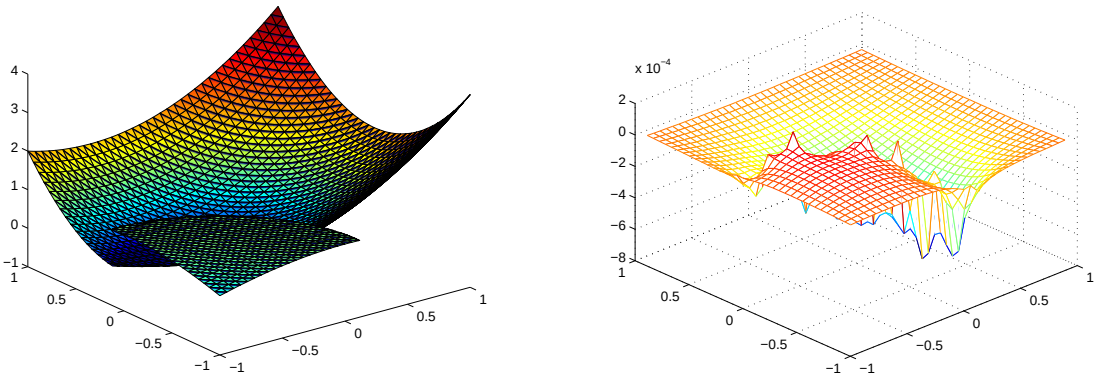
Fig. 8(a) shows the numerical result at $t = 1$ using a $36 \times 36 \times 40$ grid. Fig. 8(b) shows the error of this example at $t = 1$ using a $36 \times 36 \times 40$ grid. Table 4 shows that the method achieves 2nd order accuracy on different grids for heat equations with sharp-edged interfaces when the matrix coefficients are functions of x and y.

Example 4.5. The level-set function ϕ, the coefficients $\beta^{\pm}$ and the solution $u^{\pm}$ are

https://doi.org/10.4208/nmtma.2015.m1331 Published online by Cambridge University Press

Table 5: Quarter of a Circle

$n_x \times n_y \times n_t$	$\|u - u^h\|_\infty$	Order	$\|u_f^h - u^h\|_\infty$	Order
$9 \times 9 \times 10$	0.0097		0.0096	
$18 \times 18 \times 20$	0.0025	1.94	0.0025	1.95
$36 \times 36 \times 40$	6.19e-004	2.02	5.88e-004	2.08
$72 \times 72 \times 80$	1.61e-004	1.95	1.31e-004	2.16
$144 \times 144 \times 160$	3.82e-005	2.07		



(a) (b)

Figure 9: Quarter of a Circle.

given as follows:

$$\begin{aligned}
&\phi(x,y) = (x+1)^2 + (y+1)^2 - 1.25,\\
&\beta^+(x,y,t) = [tx^2 + 3, 0; 0, 2t + xy + 5],\\
&\beta^-(x,y,t) = [t(y+2) + 3, 0; 0, x^2/2 + y^2/2 + t/2 + 6],\\
&u^+(x,y,t) = (x^2 + 2ty^2 + xt),\\
&u^-(x,y,t) = \cos(txy).
\end{aligned}$$

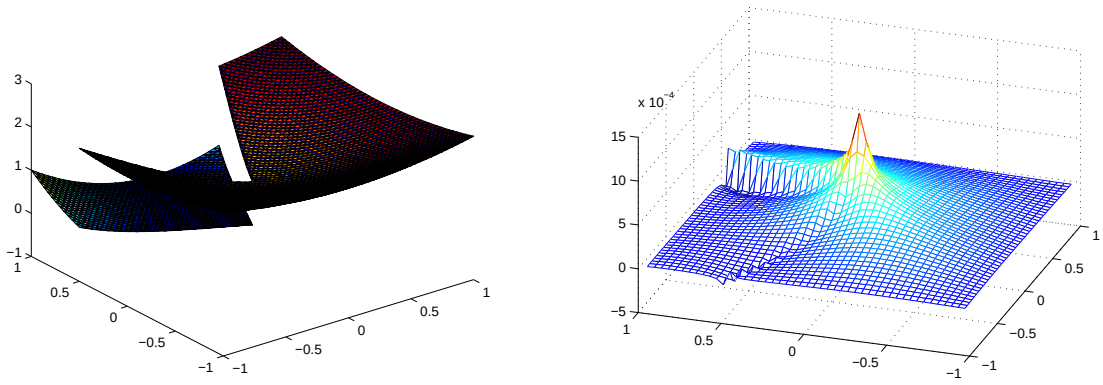
Fig. 9(a) shows the numerical result at $t = 1$ using a $36 \times 36 \times 40$ grid. Fig. 9(b) shows the error of this example at $t = 1$ using a $36 \times 36 \times 40$ grid. Table 5 shows that the method achieves 2nd order accuracy on different grids for heat equations with sharp-edged interfaces when the matrix coefficients are functions of x, y and t. Each numerical result u^h is compared with the result u_f^h, which is achieved by the finest mesh $144 \times 144 \times 160$.

Example 4.6. The solution in this example has singularity at the corner of the interface.

https://doi.org/10.4208/nmtma.2015.m1331 Published online by Cambridge University Press

Table 6: Singular point on the interface.

$n_x \times n_y \times n_t$	$\|u - u^h\|_\infty$	Order	$\|u_f^h - u^h\|_\infty$	Order
$12 \times 12 \times 10$	0.0094		0.0014	
$24 \times 24 \times 20$	0.0035	1.41	5.12e-004	1.49
$48 \times 48 \times 40$	0.0013	1.46	1.41e-004	1.86
$96 \times 96 \times 80$	4.54e-004	1.49	3.46e-005	2.03
$192 \times 192 \times 160$	1.59e-004	1.51		



(a) (b)

Figure 10: Singular point on the interface.

The level-set function ϕ, the coefficients $\beta^{\pm}$ and the solution $u^{\pm}$ are given as follows:

$$\begin{aligned}
&\phi(x,y) = y - 2x, \ \textit{if}\ x + y > 0\\
&\phi(x,y) = y + x/2, \ \textit{if}\ x + y \le 0\\
&\beta^+(x,y,t) = [x+2, 0; 0, 2+xy],\\
&\beta^-(x,y,t) = [y+2, 0; 0, 0.5(x+y)+2],\\
&u^+(x,y,t) = t^2x^2y^2,\\
&u^-(x,y,t) = (x^2+y^2)^{5/6} + \cos(xyt).
\end{aligned}$$

Fig. 10(a) shows the numerical result at $t = 1$ using a $48\times48\times40$ grid. From Fig. 10(b), we can see that the maximum error occurs at the kink where the singularity located. Table 6 shows that the method achieves almost 1.5th order accuracy on different grids for heat equations with a singular point on the sharp-edged interfaces when the matrix coefficients are functions of x and y. Each numerical result u^h is compared with the result u_f^h, which is achieved by the finest mesh $192 \times 192 \times 160$.

https://doi.org/10.4208/nmtma.2015.m1331 Published online by Cambridge University Press

5. Conclusion and future work

In this paper, we proposed a numerical method for solving the heat equations with interfaces. A weak formulation for the problem is developed and the numerical method is derived by discretizing the weak formulation. The standard finite element basis is employed for the test functions and a piecewise linear basis is constructed to satisfy the jump conditions across the interface. The modified Euler method is applied to ensure the accuracy in time. Numerical examples show that our method is second order accurate in L^∞ norm for piecewise smooth solutions and 1.5th order accurate for solutions with singularity on the sharp-edged interface. For future work, the three-dimensional problem with similar settings will be considered. Also, the conditioning of the resulting linear system of equations will be studied. Besides, for its satisfactory performance on heat equations, we are planning to extend this method to moving interface problems.

Acknowledgments The authors are grateful to the editor and referees for their valuable comments and suggestions. We thank Dr. Songming Hou of Louisiana Tech University for useful discussions. L. Wang's research is supported by Science Foundations of China University of Petroleum–Beijing (No.YJRC-2013-48, No.2462015BJB05, No.2462015YQ0604 and No.2462015QZDX02) and the Scientific Research Foundation for the Returned Overseas Chinese Scholars, State Education Ministry.

References

[1] S. M. CHADAM AND H. YIN, *A diffusion equation with localized chemical reactions*, Proc. of Edinburgh Math., vol. 37 (1993), pp. 101-118.
[2] J. D. KANDILAROV, *A Rothe-immersed interface method for a class of parabolic interface problems*, Numer. Anal. Appl., vol. 3401 (2005), pp. 328-336.
[3] C. PESKIN, *Numerical analysis of blood flow in the heart*, J. Comput. Phys., vol. 25 (1977), pp. 220-252.
[4] C. PESKIN AND B. PRINTZ, *Improved volume conservation in the computation of flows with immersed elastic boundaries*, J. Comput. Phys., vol. 105 (1993), pp. 33-46.
[5] M. SUSSMAN, P. SMEREKA, AND S. OSHER, *A level set approach for computing solutions to incompressible two-phase flow*, J. Comput. Phys., vol. 114 (1994), pp. 146-154.
[6] Z. LI, *An overview of the immersed interface method and its applications*, Taiwanese J. Math., vol. 7 (2003), pp. 1-49.
[7] R. J. LEVEQUE AND Z. LI, *The immersed interface method for elliptic equations with discontinuous coefficients and singular sources*, SIAM J. Numer. Anal., vol. 31 (1994), pp. 1019-1044.
[8] X. D. LIU, R. P. FEDKIW, AND M. KANG, *A boundary condition capturing method for Poisson's equation on irregular domains*, J. Comput. Phys., vol. 160 (2000), 151-178.
[9] R. FEDKIW, T. ASLAM, B. MERRIMAN, AND S. OSHER, *A non-oscillatory eulerian approach to interfaces in multimaterial flows (the ghost fluid method)*, J. Comput. Phys., vol. 152 (1999), 457-492.

https://doi.org/10.4208/nmtma.2015.m1331 Published online by Cambridge University Press

[10] J. W. L. Wan, and X. D. Liu, *A boundary condition capturing multigrid approach to irregular boundary problems*, SIAM J. Sci. Comput., vol. 25, no. 6 (2004), 1982-2003.
[11] P. Macklin and J. S. Lowengrub, *A new ghost cell / level set method for moving boundary problems: application to tumor growth*, J. Sci. Comput., vol. 35 (2008), pp. 266-299.
[12] S. Yu, Y. Zhou, and G. W. Wei, *Matched interface and boundary (MIB) method for elliptic problems with sharp-edged interfaces*, J. Comput. Phys., vol. 224 (2007), pp. 729-756.
[13] Y. C. Zhou, S. Zhao, M. Feig, and G. W. Wei, *High order matched interface and boundary method for elliptic equations with discontinuous coefficients and singular sources*, J. Comput. Phys., vol. 213 (2006), pp.1-30.
[14] N. Moes, J. Dolbow, and T. Belytschko, *A finite element method for crack growth without remeshing*, Int. J. Numer. Meth. Engng., vol. 46, no. 1 (1999), pp. 131-150.
[15] G. J. Wagner, N. Moes, W. K. Liu, and T. Belytschko, *The extended finite element method for rigid particles in Stokes flow*, Int. J. Numer. Meth. Engng., vol. 51, no. 3 (2001), pp. 293-313.
[16] J. Chessa and T. Belytschko, *An extended finite element method for twophase fluids: flow simulation and modeling*, J. Appl. Mech., vol. 70, no. 1 (2003), pp. 10-17.
[17] Y. Gong, B. Li, and Z. Li, *Immersed-interface finite-element methods for elliptic interface problems with non-homogeneous jump conditions*, SIAM J. Numer. Anal., vol. 46 (2008), pp. 472-495.
[18] Z. Li, T. Lin, and X. Wu, *New Cartesian grid methods for interface problems using the finite element formulation*, Numerische Mathematik, vol. 96, no. 1 (2003), pp. 61-98.
[19] I. Babuska, *The finite element method for elliptic equations with discontinuous coefficients*, Computing, vol. 5 (1970), pp. 207-218.
[20] A. Hansbo and P. Hansbo, *An unfitted finite element method, based on Nitsches method, for elliptic interface problems*, Comput. Methods Appl. Mech. Engrg., vol. 191 (2002), pp. 5537-5552.
[21] Z. Chen and J. Zou, *Finite element methods and their convergence for elliptic and parabolic interface problems*, Numer. Math., vol. 79 (1996), pp. 175-202.
[22] C. Attanayake and D. Senaratne, *Convergence of an immersed finite element method for semilinear parabolic interface problems*, Appl. Math. Sci., vol. 5, no. 3 (2011), pp. 135-147.
[23] S. Hou and X. D. Liu, *A numerical method for solving variable coefficient elliptic equations with interfaces*, J. Comput. Phys., vol. 202 (2005), pp. 411-445.
[24] S. Hou, W. Wang, and L. Wang, *Numerical method for solving matrix coefficient elliptic equation with sharp-edged interfaces*, J. Comput. Phys., vol. 229 (2010), pp. 7162-7179.
[25] S. Hou, P. Song, L. Wang, and H. Zhao, *A weak formulation for solving elliptic interface problems without body fitted grid*, J. Comput. Phys., vol. 249 (2013), pp. 80-95.
[26] H. Johansen and P. Colella, *A cartesian grid embedded boundary method for poisson's equation on irregular domains*, J. Comput. Phys., vol. 147 (1998), pp. 60-85.
[27] P. McCorquodale, P. Colella, and H. Johansen, *A cartesian grid embedded boundary method for the heat equation on irregular domains*, J. Comput. Phys., vol. 173 (2001), pp. 620-635.
[28] P. Schwartz, M. Barad, P. Colella, and T. Ligocki, *A cartesian grid embedded boundary method for the heat equation and poisson's equation in three dimensions*, J. Comput. Phys., vol. 211 (2006), pp. 531-550.
[29] S. Wang, R. Samulyak, and T. Guo, *An embedded boundary method for elliptic and parabolic problems with interfaces and application to multi-material systems with phase transitions*, Acta Mathematica Scientia, vol. 30, no.2 (2010), pp. 499-521.

https://doi.org/10.4208/nmtma.2015.m1331 Published online by Cambridge University Press

[30] S. HOU, Z. LI, L. WANG, AND W. WANG, *A numerical method for solving elasticity equations with interfaces*, Comm. Comput. Phys., vol. 12 (2012), pp. 595-612.
[31] S. HOU, L. WANG, AND W. WANG, *A numerical method for solving the elliptic interface problems with multi-domains and triple junction points*, J. Comput. Math., vol. 30 (2012), pp. 504-516.
[32] L. WANG, S. HOU, AND L. SHI, *A numerical method for solving 3D elasticity equations with sharp-edged interfaces*, Int. J. PDE., (2013) Article ID 476873.
[33] L. WANG AND L. SHI, *Numerical method for solving matrix coefficient elliptic equations in irregular domain with sharp-edged boundary*, Adv. Numer. Anal., (2013) Article ID 967342.
[34] L. WANG, S. HOU, AND L. SHI, *An improved non-traditional finite element formulation for solving the elliptic interface problems*, J. Comput. Math., vol. 32 (2014), pp. 39-57.
[35] L. WANG AND L. SHI, *A simple method for matrix-valued coefficient elliptic equations with sharp-edged interfaces*, Appl. Math. Comput., vol. 242 (2014), pp. 917-930
[36] Z. LI AND Y. SHEN, *A numerical method for solving heat equations involving interfaces*, Electron. J. Diff. Eqns., Conf. 03 (1999), pp. 100-108.
[37] J. HUANG AND J. ZOU, *Some New A Priori Estimates for Second-Order Elliptic and Parabolic Interface Problems*, J. Diff. Eqns., vol. 184 (2002), pp. 570-586.
[38] X. YANG, B. LI, AND Z. LI, *The Immersed Interface Method for Elasticity Problems with Interfaces*, Dyn. Contin. Discrete Impuls. Syst. Ser. A Math. Anal., 10/2003.
[39] W. DAI, A. KHALIQ, AND R. NASSAR, *An Introduction to Finite Element Mtehod*, Louisiana Tech University Text Book, Ruston, Louisiana, USA.
[40] J. NECAS, *Introduction to the theory of nonlinear elliptic equations*, Teubner-Texte zur Mathematik, Band 52 (1983), ISSN 0138-502X.

https://doi.org/10.4208/nmtma.2015.m1331 Published online by Cambridge University Press